Transition to Linear Domain Walls in Nanoconstrictions

N. Kazantseva, R. Wieser, and U. Nowak
Fachbereich Physik, Universität Duisburg-Essen, 47048 Duisburg, Germany
(Received 25 August 2004; published 27 January 2005)

Domain walls in nanoconstrictions are investigated with a focus on thermal properties. In general, the magnetization component perpendicular to the easy axis which in a domain wall usually occurs has a value different from the easy-axis bulk magnetization value with a separate phase transition at a critical temperature below the Curie temperature. Since this effect is the more pronounced the smaller the domain wall width is, we investigate it especially in domain walls with a confined geometry, using analytical arguments, mean-field theory, and Monte Carlo simulations. Our findings may contribute to the understanding of magnetoresistive effects in domain walls with sizes of only a few atomic layers, as, e.g., in nanocontacts or nanoconstrictions.

DOI: 10.1103/PhysRevLett.94.037206 PACS numbers: 75.60.Ch, 75.10.Hk, 75.47.Jn, 75.75.+a

Well controlled domain walls could become important constituents of future magnetoelectronic devices [1]. Especially, the understanding of domain walls in confined nanometric geometries is important since those can show behavior deviating from their usual bulk properties, as, e.g., a controlled pinning and a strongly reduced domain wall width [2–5]. The latter is thought to contribute to large magnetoresistance effects of domain walls in nanowires [6], nanoconstrictions [7], and nanocontacts [8,9].

In only a few publications the temperature dependence of domain wall properties was investigated [10–12]. Most important in this context is the pioneering work of Bulaevskiĭ and Ginzburg [13] who showed within the framework of Ginzburg-Landau theory that for a one dimensional domain wall profile (e.g., a Bloch wall) the easy-axis and hard-axis components of the magnetization, respectively, are two separate order parameters with different critical temperatures. In other words, the perpendicular magnetization component which arises necessarily in a domain wall has at finite temperatures values lower than the easy-axis equilibrium magnetization (leading to the term ''elliptical domain walls'') and vanishes completely for a temperature T_h which is lower than the Curie temperature T_c of the bulk material (leading to the term ''linear domain walls'' for temperatures $T_h < T < T_c$).

However, the deviation of T_h from T_c is proportional to the squared inverse domain wall width [13] and, hence, should be very small. Consequently, linear walls are hard to detect experimentally [14]; their relevance is considered to be rather low and most of the numerical calculations of domain wall properties are performed using micromagnetic codes where the assumption of a constant magnetization value is made in contradiction to the findings described above. In the following we investigate how far thermodynamic deviations from pure Bloch-like domain wall structures can become relevant due to the reduced size of domain walls in confined geometries. This is an important issue since it was suggested [15] that linear domain walls might explain the observed large magnetoresistance effects in constrained domain walls.

In the following we consider a domain wall structure as shown in Fig. 1. In the picture, each arrow represents the mean magnetization of a plane. Our Monte Carlo (MC) simulations are for a full three dimensional model allowing for magnetization fluctuations within the planes while in the mean-field (MF) approximation each (infinite) plane is represented as one magnetization vector so that the model is effectively one dimensional. Depending on the details of the methods we apply, we use either fixed boundary conditions where the first and the last plane of the system are fixed as shown in the figure or we use antiperiodic boundary conditions. In both cases we force a domain wall into the system which for a large system size (number of planes N) will not fill up the whole system. However, for a smaller system size the boundary conditions force the domain wall to adopt the system size. This models a domain wall caught in a nanoconstriction [2] where perfect pinning is assumed.

We investigate the system in terms of a classical spin model with spin variables $|\boldsymbol{S}_i| = 1$ on a cubic lattice with lattice constant a and energy contributions from ferromagnetic exchange between nearest neighbors with coupling constant J and a uniaxial anisotropy with $D > 0$ defining the easy axis of the system,

$$\mathcal{H} = -\frac{J}{2}\sum_{\langle i,j\rangle} \boldsymbol{S}_i \cdot \boldsymbol{S}_j - D\sum_i (S_i^e)^2. \qquad (1)$$

In the zero-temperature limit all spins within a plane will be parallel and the domain wall profiles can be calculated

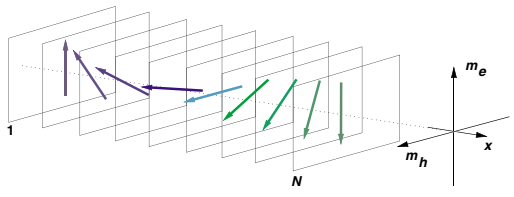

FIG. 1 (color online). Sketch of the wall geometry. The magnetization of the first and the last plane are antiparallel along the easy axis. The magnetization rotates in a plane via the hard axis.

analytically in the continuum limit where the energy density (per cross-sectional area) is a one dimensional integral

$$e = \frac{J}{2a}\int_{-L/2}^{L/2}(\nabla\cdot\mathbf{S})^2 dx - \frac{D}{a^3}\int_{-L/2}^{L/2}(S^e)^2 dx.$$

The magnetization of the domain wall rotates within a plane and can be expressed by a single angle of rotation θ. The Euler-Lagrange equation which minimizes the energy above is solved by an elliptic integral

$$x = \int_{-\pi/2}^{\phi}\frac{\delta_0 d\theta}{\sqrt{c^2-\sin^2\theta}} = \frac{\delta_0}{c}F\left(\phi,\frac{1}{c^2}\right),$$

where $\delta_0 = a\sqrt{J/2D}$ is the zero-temperature domain wall width of an unconstrained wall and the integration constant c is given by the boundary condition $x(\pi/2) = L/2$ with $L = (N-1)a$. The wall profiles are then given by Jacobian sine and cosine functions

$$S_e(x) = \mathrm{sn}\left(\frac{cx}{\delta_0},\frac{1}{c^2}\right); \qquad S_h(x) = \mathrm{cn}\left(\frac{cx}{\delta_0},\frac{1}{c^2}\right). \quad (2)$$

The limit $c \to 1$ corresponds to an unconstrained wall with the usual Bloch-wall profiles

$$S_e(x) = \tanh(x/\delta_0); \qquad S_h(x) = \cosh^{-1}(x/\delta_0). \quad (3)$$

The opposite case, $c \gg 1$, corresponds to a very constrained wall ($L \ll \delta_0$) where the wall is forced to adapt the system size and the profiles follow simple trigonometric functions,

$$S_e(x) = \sin(\pi x/L); \qquad S_h(x) = \cos(\pi x/L). \quad (4)$$

In this limit the actual domain wall width is L.

As an example, Fig. 2 shows a comparison of these expressions with numerical MF results, obtained as described below in the low temperature limit $k_B T = 0.02J$. The smaller system shows the case of a very constrained wall where the wall profiles are already described by trigonometric functions while the larger system shows an intermediate case. Note that in Ref. [2] corresponding calculations were made, but for other boundary conditions and system geometries, respectively.

However, we want to focus on thermal properties and in order to obtain results for finite temperatures we start with the MF Hamilton operator which (neglecting terms without $\boldsymbol{S}$) is

$$\mathcal{H}_{\mathrm{MF}} = -\sum_i [J\boldsymbol{S}_i\cdot(\boldsymbol{m}_{i-1}+4\boldsymbol{m}_i+\boldsymbol{m}_{i+1}) + D(S_i^e)^2], \quad (5)$$

where the contribution $4\boldsymbol{S}_i\cdot\boldsymbol{m}_i$ comes from the four neighbors within the plane. Then we solve the MF self-consistency equations,

$$\mathbf{m}_i = \langle\mathbf{S}_i\rangle = \frac{1}{Z}\mathrm{Tr}\mathbf{S}_i e^{-\mathcal{H}_{\mathrm{MF}}/k_B T}$$

with $Z = \mathrm{Tr}e^{-\mathcal{H}_{\mathrm{MF}}/k_B T}$ numerically. Here, $\mathbf{m}_i$ is the thermally averaged magnetization of the ith plane and the trace is an integral over the unit sphere. These equations can be solved iteratively, starting with an arbitrary magnetization profile and then let the equations evolve until a stationary state is reached.

Let us start with the case of an unconstrained wall. Figure 3 shows domain wall profiles for two different temperatures where the system size $L = 40a$ is large enough so that an equilibrium domain wall for an anisotropy value of $D = 0.03J$ fits well into the system. The solid lines are the analytical functions as calculated above, here, simply the tanh and $1/\cosh$ profiles. Interestingly, for finite temperatures the mathematical form of the wall profile is conserved; solely the amplitudes and the domain wall widths vary with temperature. Hence, in the limit $L \gg \delta_0$ the thermodynamic wall profiles can be described as in Eqs. (3) but with a temperature dependent domain wall width $\delta(T)$ and temperature dependent amplitudes $M_h(T)$ and $M_e(T)$. Furthermore, Fig. 3 suggests that the temperature dependence of the two amplitudes is not the same.

Instead, these amplitudes, M_h and M_e, define two distinct order parameters as shown in Fig. 4. Obviously, these two order parameters vanish continuously at two different temperatures where the upper one is the usual Curie tem-

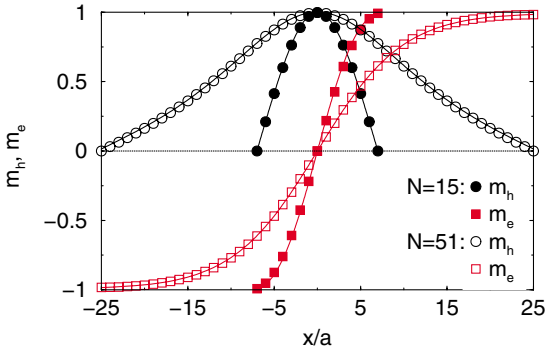

FIG. 2 (color online). Ground state easy- and hard-axis magnetization profiles for constrained walls. Data points are from low temperature MF calculations; solid lines correspond to Eq. (2). $D/J = 0.003$.

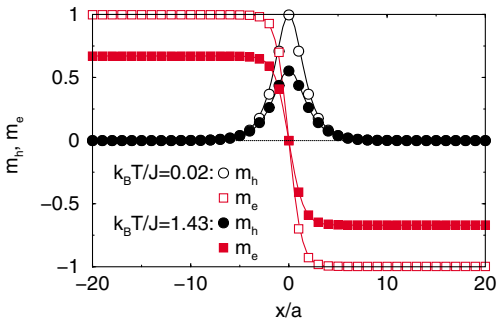

FIG. 3 (color online). Easy- and hard-axis magnetization profiles in MF approximation for two different temperatures. $D/J = 0.03$.

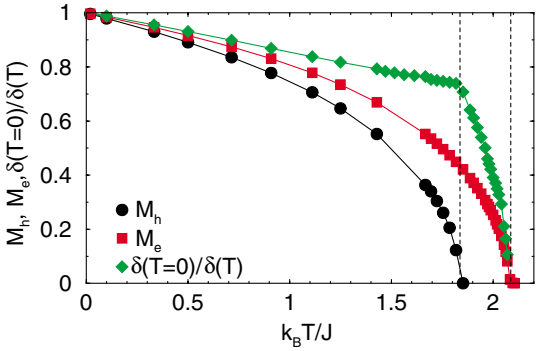

FIG. 4 (color online). Temperature dependence of easy- and hard-axis order parameters and (reduced) inverse domain wall width from MF calculations. $L = 50a$, $D/J = 0.3$.

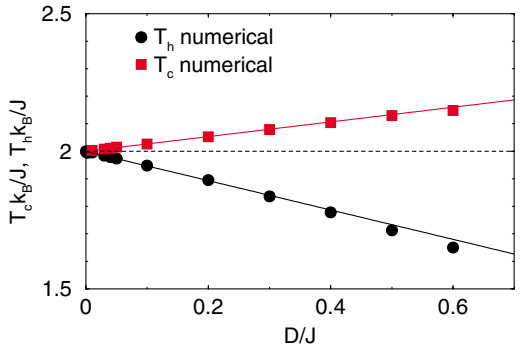

FIG. 5 (color online). Anisotropy dependence of the two critical temperatures T_c and T_h. Data points are from MF calculations as in Fig. 4, solid lines from Eq. (6).

perature T_c and the lower one is a second critical temperature, T_h, which describes the phase transition of the hard-axis component of the magnetization vector. For temperatures $T_h < T < T_c$ the domain wall is linear with an easy-axis component of the magnetization only. For $T < T_h$ in general one finds an elliptical wall profile which for lower temperature goes over to the usual Bloch-wall profile. Also shown in Fig. 4 is the reduced, inverse domain wall width demonstrating that $\delta(T)$ increases slightly with temperature for elliptical domain walls, shows a kink at T_h, and then diverges in the linear wall regime approaching T_c.

Both critical temperatures depend on the strength of the anisotropy D as is shown in Fig. 5. T_c corresponds to the usual bulk Curie temperature and its anisotropy dependence expanded with respect to D/J is $k_B T_c/J = 2 + \frac{4}{15} D/J + \mathcal{O}[D/J]^2$. As Fig. 5 demonstrates, T_h has also a linear dependence on D/J in the range of anisotropies which is shown in the figure, and our numerical results suggest $k_B T_h/J \approx 2 - 0.53 D/J$. This means that the difference between both critical temperatures scales with the squared inverse domain wall width

$$k_B(T_c - T_h)/J \approx 0.40 a^2/\delta_0^2. \tag{6}$$

These findings, the second phase transition, its dependence on δ_0, and the diverging domain wall width are qualitatively in agreement with the earlier calculation within the framework of the Ginzburg-Landau theory [13]—an expansion close to T_c—where it was also shown that close to T_c the (linear) wall has a tanh profile. However, for experimental systems reasonable anisotropies are rather small, so that in general the two critical temperatures should nearly coincide and M_h should be close to the easy-axis magnetization M_e. Nevertheless, experimental investigations of linear domain walls exist. In [14] the influence of the wall structure (either elliptical or linear) on the domain wall mobility was investigated. Here, the deviation of T_h from T_c was 1%. However, since, as Eq. (6) shows, these effects increase with decreasing domain wall width larger effects should occur in smaller domain walls as found, e.g., in constrained geometries.

For a strongly constrained domain wall and in MF approximation T_h can be estimated analytically. For a system with antiperiodic boundary conditions and small anisotropy, so that $L \ll \delta_0$, the wall profiles follow trigonometric functions which means that the angle of rotation from plane to plane changes in each plane by the same amount $\pi a/L$. This leads to a decrease of the MF coming from the two adjacent planes proportional to $\cos(\pi a/L)$. Including this in the MF Hamiltonian [Eq. (5)] the critical temperature for zero anisotropy can be calculated in the usual way, now leading to

$$k_B T_h/J = \frac{4}{3} + \frac{2}{3}\cos\left(\frac{\pi a}{L}\right). \tag{7}$$

Note that for a constrained domain wall with $L \ll \delta_0$ much bigger effects may occur than before [Eq. (6)].

In Fig. 6 we compare the formula above with numerical calculations for the case of constrained walls. We use $D = 0$, so that the condition $L \ll \delta_0$ is always fulfilled, and simulate systems with fixed boundary conditions calculating T_h from the hard-axis magnetization. Figure 6 demon-

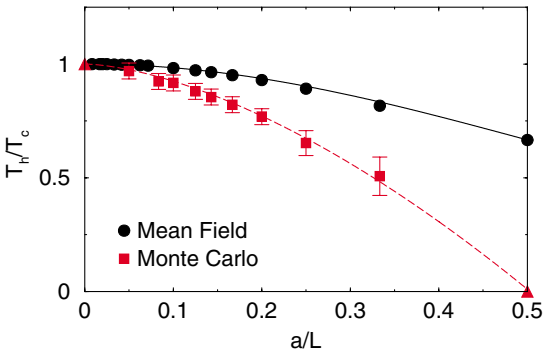

FIG. 6 (color online). Dependence of the critical temperature T_h from the size of the constrained domain wall. Comparison of MC data, MF calculations, and Eq. (7) (solid line). The dashed line is a guide to the eye.

strates that pronounced effects can be found when the domain wall is constrained to only a few atomic layers. The agreement of our MF data with Eq. (7) is very good. Nevertheless, the MF approximation strongly underestimates this size dependent effect: this can be concluded from the fact that even in the extreme case of a three layer system—which is due to the fixed boundary condition corresponding to a free monolayer—a finite T_h is found even though it is clear from the Mermin-Wagner theorem that no order should occur.

Therefore, we additionally used MC methods to investigate the breakdown of ferromagnetic order in the original spin model [Eq. (1)] more rigorously. Using MC methods thermal excitations (thermally excited spin waves) are fully taken into account. We use a heat-bath algorithm and single-spin-flip dynamics for the simulations. At every MC step each spin is subject to a trial step consisting of a small deviation from the original direction [16]. The lateral dimension of the system is up to 128×128 with periodic boundary conditions. The number of planes is varied from 3 to 21 where we use fixed boundary conditions for the first and last planes. We start the simulations with an abrupt domain wall and let it relax for 10 000 MCS (MC steps per spin). Then we calculate the absolute value of the magnetization component perpendicular to the easy axis, averaged over the whole system and for another 100 000 MCS as order parameter of the phase transition. Note that the precise definition of the order parameter is important: without calculating the absolute value of the perpendicular magnetization the long time average of one magnetization component will always be zero since the wall magnetization might rotate in the hard plane. Furthermore, to average over the whole system is also important since the wall can move diffusively.

T_h is then determined from a finite-size scaling analysis of the order parameter above where the lateral system size is varied from 8×8 to 128×128. The resulting data points are also shown in Fig. 6. The scaling analysis works well with the exponents β and ν from the three dimensional Heisenberg model. Only for a very small number of planes deviations occur indicating a crossover from three to two dimensional behavior [17]. As expected T_h now goes to zero in the limiting case of a trilayer system so that the change of the critical temperature is more dramatic. For example, for a wall consisting of five atomic planes ($L = 4a$) T_h is reduced by about 35% as compared to the Curie temperature and even for a temperature of $0.5T_c$ the hard-axis magnetization (the degree of order within the wall) is reduced by about 20% as compared to the easy-axis bulk value.

To summarize, investigating the influence of thermal activation on the properties of domain walls in nanoconstrictions we have demonstrated that with increasing temperature Bloch-wall profiles change via elliptical walls to linear domain walls. The temperature range where these effects occur scales with the squared inverse domain wall width so that in general it is rather small. However, since in confined geometries the relevant quantity is the size of the constriction larger effects can be found. The breakdown of ferromagnetic order is due to the fact that in a domain wall the mean exchange field decreases due to the finite angle of rotation between neighboring magnetic moments. Hence, it is a general effect which will also occur in other types of domain walls as, e.g., vortex walls. Our findings may have an impact on the understanding of domain wall magnetoresistance properties [15,18–20], especially its temperature dependence, for two reasons: first, in an elliptical or linear domain wall the degree of spin disorder is larger in the wall than in the bulk of the domain since the value of the order parameter is lower. Second, as suggested in [15], in a linear domain wall the change of the magnetization direction is abrupt while only its value is changing. This means that the spin of a conductance electron passing a linear wall cannot follow a continuously rotating magnetization direction.

The authors thank R. W. Chantrell, A. Hucht, and K. D. Usadel for stimulating discussions. This work was supported by the *Deutsche Forschungsgemeinschaft* (SFB 491).

[1] D. A. Allwood *et al.*, Science **296**, 2003 (2002).
[2] P. Bruno, Phys. Rev. Lett. **83**, 2425 (1999).
[3] O. Pietzsch, A. Kubetzka, M. Bode, and R. Wiesendanger, Phys. Rev. Lett. **84**, 5212 (2000).
[4] K. Miyake *et al.*, J. Appl. Phys. **91**, 3468 (2002).
[5] M. Kläui *et al.*, Phys. Rev. Lett. **90**, 097202 (2003).
[6] U. Ebels *et al.*, Phys. Rev. Lett. **84**, 983 (2000).
[7] C. Rüster *et al.*, Phys. Rev. Lett. **91**, 216602 (2003).
[8] N. Garcia, N. Munoz, and Y.-W. Zhao, Phys. Rev. Lett. **82**, 2923 (1999).
[9] H. D. Chopra and S. Z. Hua, Phys. Rev. B **66**, 020403 (2002).
[10] D. A. Garanin, Physica (Amsterdam) **178A**, 467 (1991).
[11] Y. Labaye, L. Berger, and J. M. D. Coey, J. Appl. Phys. **91**, 5341 (2002).
[12] J. M. D. Coey, L. Berger, and Y. Labaye, Phys. Rev. B **64**, 020407 (2003).
[13] L. N. Bulaevskiĭ and V. L. Ginzburg, Sov. Phys. JETP **18**, 530 (1964).
[14] J. Kötzler, D. A. Garanin, M. Hartl, and L. Jahn, Phys. Rev. Lett. **71**, 177 (1993).
[15] M. Dzero, L. P. Gor'kov, A. K. Zvezdin, and K. A. Zvezdin, Phys. Rev. B **67**, 100402 (2003).
[16] U. Nowak, in *Annual Reviews of Computational Physics IX*, edited by D. Stauffer (World Scientific, Singapore, 2001), p. 105.
[17] D. A. Garanin, J. Phys. A **29**, 2349 (1996).
[18] P. M. Levy and S. Zhang, Phys. Rev. Lett. **79**, 5110 (1997).
[19] B. Y. Yavorsky *et al.*, Phys. Rev. B **66**, 174422 (2002).
[20] F. S. Bergeret, A. F. Volkov, and K. B. Efetov, Phys. Rev. B **66**, 184403 (2003).